MIT ESD

Massachusetts Institute of Technology
Engineering Systems Division

ESD Working Paper Series

Airport Congestion Mitigation through Dynamic Control of Runway Configurations and of Arrival and Departure Service Rates under Stochastic Operating Conditions

Alexandre Jacquillat
Massachusetts Institute of Technology
Cambridge, MA 02139
alexjacq@mit.edu

Mort D. Webster
Massachusetts Institute of Technology
Cambridge, MA 02139
mort@mit.edu

Amedeo R. Odoni
Massachusetts Institute of Technology
Cambridge, MA 02139
arodoni@mit.edu

ESD-WP-2013-14

July 2013
updated May 2014

esd.mit.edu/wps

Airport Congestion Mitigation through Dynamic Control of Runway Configurations and of Arrival and Departure Service Rates under Stochastic Operating Conditions

Alexandre Jacquillat Amedeo R. Odoni
Mort D. Webster
Massachusetts Institute of Technology, Cambridge, MA 02139
alexjacq@mit.edu, arodoni@mit.edu, mort@mit.edu

Abstract

The high levels of flight delays require the implementation of airport congestion mitigation tools. In this paper, we optimize the utilization of airport capacity at the tactical level in the face of operational uncertainty. We formulate an original Dynamic Programming model that selects jointly and dynamically runway configurations and the balance of arrival and departure service rates at a busy airport to minimize congestion costs, under stochastic queue dynamics and stochastic operating conditions. The control is exercised as a function of flight schedules, of arrival and departure queue lengths and of weather and wind conditions. We implement the model in a realistic setting at JFK Airport. The exact Dynamic Programming algorithm terminates within reasonable time frames. In addition, we implement an approximate one-step look-ahead algorithm that considerably accelerates the execution of the model and results in close-to-optimal policies. In combination, these solution algorithms enable the on-line implementation of the model using real-time information on flight schedules and meteorological conditions. The application of the model shows that the optimal policy is path-dependent, *i.e.*, it depends on prior decisions and on the stochastic evolution of arrival and departure queues during the day. This underscores the theoretical and practical need for integrating operating stochasticity into the decision-making framework. From comparisons with an alternative model based on deterministic queue dynamics, we estimate the benefit of considering queue stochasticity at 5% to 20%. Finally, comparisons with advanced heuristics aimed to imitate actual operating procedures suggest that the model can yield significant cost savings, estimated at 20% to 30%.

Key words Airport, Capacity, Delay, Runway Configuration, Dynamic Programming, Queuing Model

1 Introduction

Airport congestion is an increasingly important and costly phenomenon worldwide. In the United States, air traffic delays reached an all-time peak in 2007 and their nationwide impact was estimated

at over $30 billion for that calendar year [1]. Most of these delays are caused by mismatches between demand and capacity resulting from airlines scheduling more flights than realized capacity at the airports. In recent years, an estimated 50% to 75% of system-wide delays can be attributed to heavy traffic volume, capacity shortages related to non-extreme weather conditions, inefficiencies in airport operations and the propagation of schedule disturbances within the network of airline operations [6].

Significant delay reductions in the United States can therefore be achieved by reducing the imbalance between demand and capacity at the busiest airports. Medium-term and long-term options include capacity expansion and demand management. Capacity expansion can be achieved through infrastructure expansion, including the construction of new airports or new runways [7], or through improvements in air traffic management technologies, such as the development of the Next Generation Air Transportation System (NextGen) [11]. However, such projects require extensive investments and many years to plan and implement. More importantly, they might be infeasible in the most densely populated areas. Demand management aims to reduce peak-hour scheduling levels through slot limits or congestion pricing. Such mechanisms could lead to significant delay reductions [25] and could provide operational benefits to air carriers and passengers [31, 30]. However, the implementation of these measures has been limited in the United States due to the opposition they typically engender from air carriers, which are concerned about any constraints on flight schedules such measures would impose.

This paper examines an alternative approach to reducing demand-capacity mismatches, consisting of improvements in the *utilization* of airport capacity at the tactical level. Airport throughput depends on the runway configuration in use, *i.e.*, the set of active runways on which landings and takeoffs are operated, and on the relative proportion of landings and takeoffs [28]. For any schedule of flights on a given day, airport congestion can thus be mitigated through improvements in the control of runway configurations and in balancing arrival and departure service rates. In practice, these are two of the major decisions faced by air traffic controllers and they are primarily made on the basis of experience. The main drivers of these decisions include inertia, wind speed and directions, arrival and departure schedules, noise abatement procedures, configuration switch proximity and inter-airport coordination [27]. This paper develops a decision support tool to improve the selection of runway configurations and the balancing of arrival and departure service rates including, for the first time, the consideration of the stochasticity of airport operations in these decisions.

The optimization of airport capacity utilization is an important topic in Air Traffic Flow Management. Gilbo [12, 13] was the first to explicitly consider the problem of optimally allocating airport capacity between arrivals and departures given the non-increasing relationship between arrival capacity and departure capacity represented by means of a piecewise linear *Capacity Envelope*. This framework was later extended to account for general Capacity Envelopes and nonlinear objective functions [8] and at the multi-airport level in the development of Ground Delay Programs

[15, 14].

More recent studies addressed the problem of *jointly* selecting runway configurations and arrival and departure service rates by introducing different Capacity Envelopes for different runway configurations. Optimizing these decisions jointly is critical when different runway configurations achieve different arrival and departure throughput. This may occur if, for instance, a particular configuration allocates one runway to arrivals and two runways to departures, while an alternative configuration allocates two runways to arrivals and one to departures. Bertsimas et al. [5] developed a Mixed Integer Program that determines the optimal schedule of runway configurations and of arrival and departure service rates for an entire day of operations. This model was extended to account for marginally decreasing penalties associated with runway configuration switches [32]. Li and Clarke [20] developed an alternative formulation that dynamically controls runway configurations under stochastic wind conditions. This literature has demonstrated that the optimal selection of runway configurations and of the arrival/departure balance can lead to significant congestion cost savings. All existing approaches consider deterministic queue dynamics.

In contrast, airport operations have been extensively described by means of *stochastic* queuing models [19, 24, 23]. The stochasticity in these models aims to capture the uncertainty and variability of the dynamics of formation and propagation of airport queues. Indeed, queues do not depend solely on the schedule of flights and the availability of airport capacity, but are also shaped by the exact sequencing of arrivals and departures, by the mix of aircraft, by human factors in aircraft operations, etc. Dynamic and stochastic queuing models of airport congestion were shown to approximate accurately the extent of congestion observed at the busiest US airports [22, 26, 17] and to provide higher estimates of flight delays than deterministic models [16]. Moreover, exogenous variables, such as weather and winds, are also stochastic and directly impact airport operations: winds constrain the set of runways that can be used at any time, while cloud ceiling and visibility influence the efficiency of airport operations.

In this paper, we formulate and solve the problem of selecting runway configurations and the balance of arrival and departure service rates under stochastic queue dynamics and stochastic operating conditions, including weather and winds. This paper thus intends to bridge the gap in the literature between descriptive stochastic models of airport congestion and optimization models of capacity utilization based on deterministic queue dynamics. Under stochastic airport operations, the arrival and departure queues observed at later time periods are *not* known with certainty in advance. We thus develop a *dynamic* decision-making framework. For instance, let us consider a period of the day when more arrivals than departures are scheduled. Traditional approaches might suggest the use of a runway configuration that gives priority to arrivals over departures during that period. If, however, the departure queue is longer than expected at the beginning of the period, while the arrival queue is shorter than expected, then it might be beneficial to choose an alternative runway configuration to enhance the departure throughput and alleviate ground congestion. A

dynamic approach might thus yield operational benefits in the face of queue uncertainty.

Any decision-making support tool must be applicable in real time. Indeed, airport operations are subject to real-time disturbances that might impact operating procedures. This might include schedule updates arising from the occurrence of upstream delays in previous flight legs, en-route congestion or changes in scheduled departures at other airports when a Ground Delay Program is initiated. This might also include changes in weather and wind forecasts. For this reason, we develop a solution architecture that enables the dynamic revision of operating policies. Such revisions are performed almost instantaneously as new real-time information becomes available and are thus well suited to the actual problem faced by air traffic controllers.

The contributions of this paper fall into four categories presented in § 2 through § 5:

- In § 2, we formulate an original Dynamic Programming (DP) model that selects jointly and dynamically runway configurations and the balance of arrival and departure service rates at a busy airport to minimize congestion costs, under stochastic queue dynamics and stochastic operating conditions. The model takes as inputs capacity estimates and the schedule of flights. At each period of the day, decisions are based on (i) the arrival queue length, (ii) the departure queue length, (iii) the runway configuration previously in use, (iv) weather conditions and (v) wind conditions.

- In § 3, we present exact and approximate solution algorithms that, in combination, enable the on-line implementation of a 2-step optimization approach that uses *a priori* as well as real-time information. In the first step, the exact DP model of § 2 provides operating policies for an entire day of operations, based on inputs available before the beginning of that day. However, this policy might no longer be optimal in the face of such operating disturbances as schedule updates and updated weather forecasts. We therefore implement, as a second step, a fast approximate algorithm based on a one-step look-ahead that greatly accelerates the execution of the DP model. Computational experiments show that this 2-step approximation scheme yields congestion costs within 2% of the optimal solution and thus results in close-to-optimal policies.

- In § 4, we describe a detailed application of our approach to the John F. Kennedy International Airport (JFK). We show that the optimal policy is path dependent, *i.e.*, depends on prior decisions and on the prior stochastic evolution of the system over the day. This underscores the theoretical and practical need for integrating operating stochasticity into the decision-making framework.

- In § 5, we show that the model can result in significant congestion cost savings at busy airports, as compared to current operating procedures and existing approaches in the literature. First, we compare the model to two advanced heuristics that aim to imitate typical decisions made in practice. We estimate the resulting congestion cost savings at 20% to 30%. Second, we

compare the model to an alternative model based on deterministic queue dynamics and we estimate the benefit of integrating queue stochasticity into the decision-making framework at 5% to 20%.

2 Model Formulation

We formulate the dynamic control of runway configurations and of arrival and departure service rates as a finite-horizon Dynamic Programming (DP) model. A day of operations, between 6 a.m. and midnight, is divided into $T = 72$ periods of length $S = 15$ minutes. We index these time periods by $t = 1, ..., T$. Observations and decisions are made at the beginning of each period. Operations between midnight and 6 a.m. are not considered since they are typically not capacity-constrained and decisions are based on noise abatement procedures and other environmental concerns.

2.1 Problem Statement

The model takes as inputs (a) the schedule of landings and takeoffs on a given day and (b) estimates of the capacity of each runway configuration. During each 15-minute period of the day, we denote by x_t (resp. y_t) the number of aircraft scheduled to land (resp. to take off) at the considered airport. We represent the capacity of each runway configuration by means of an *Operational Throughput Envelope*, which characterizes the non-increasing relationship between the *average* arrival rate and the *average* departure rate in the presence of continuous demand, for the runway configuration considered [28]. This representation takes into account the variability of the traffic mix, including different aircraft types, different sequencing of arrivals and departures, etc. Since airport operations are substantially impacted by weather conditions, we specify one Operational Throughput Envelope for each runway configuration in "Visual Meteorological Conditions" (VMC) and another one in "Instrument Meteorological Conditions" (IMC)—we use VMC and IMC as surrogates of "good" and "poor" weather conditions, respectively.

A schematic representation of the model's inputs is provided in Figure 1. In this figure, each dot represents a hypothetical count of scheduled arrivals and departures per time period (*i.e.*, per 15 minutes). We also show the VMC and IMC Operational Throughput Envelopes associated with two hypothetical runway configurations that achieve different trade-offs between arrival and departure capacity—Configuration 1 can achieve the largest arrival throughput when few departures are operated while Configuration 2 achieves the largest departure throughput. Two immediate observations are noteworthy. First, a larger average throughput can be achieved in VMC than in IMC. Second, the relationship between the arrival service rate and the departure service rate for a given runway configuration is non-increasing.

The problem of jointly selecting a configuration and the arrival and departure service rates, under dynamic and stochastic conditions, can be illustrated as follows. Let us consider a period of the

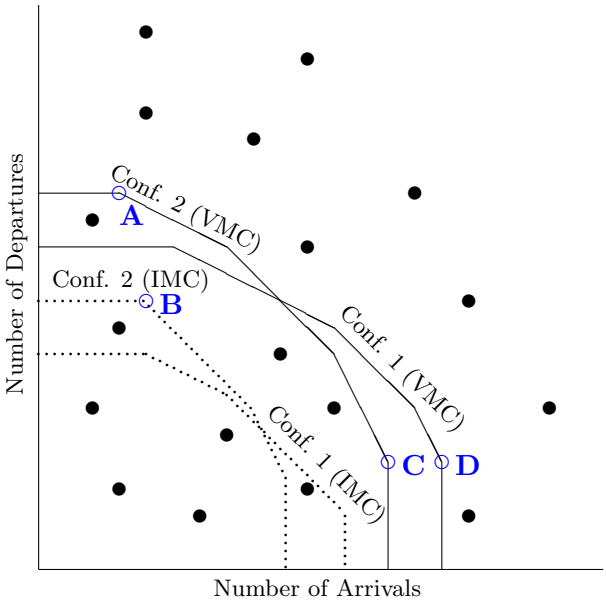

Figure 1: Schematic representation of VMC and IMC Operational Throughput Envelopes

day with a large number of scheduled departures. It might be optimal to operate in Configuration 2 during this period, in order to achieve a large departure throughput (*e.g.*, by operating with the service rates corresponding to Point A in VMC or to Point B in IMC). If, at a later period, a large number of arrivals are expected to be operated, then it might be optimal to enhance the arrival throughput. This can be done by staying in Configuration 2 (*e.g.*, by operating in Point C) or by switching to Configuration 1 to increase the arrival throughput further (*e.g.*, by operating in Point D). The best choice is not obvious for at least two reasons. First, there is a trade-off between the potential efficiency enhancements resulting from configuration switches and the costs of operational inefficiency during the time it takes to switch configurations. Second, the stochasticity of airport operations makes it challenging to anticipate the future evolution of the system.

2.2 State Variables

The decisions in each period depend on the observed extent of congestion, on the runway configuration in use and on operating conditions. Operating conditions, including weather and winds, are assumed to be observed at the beginning of each time window and not to change over one 15-minute period. At the beginning of period t, the state is described by the following variables:

- Arrival Queue Length a_{t-1}: Number of arriving aircraft queuing in the air at the end of the previous period
- Departure Queue Length d_{t-1}: Number of departing aircraft queuing on the ground at the end of the previous period

- The runway configuration in use at period $t-1$, denoted by RC_{t-1}
- Weather conditions for the next period, denoted by $wc_t \in \{VMC, IMC\}$
- The wind state ws_t, which determines the set of runway configurations that *can* be used at any time. According to FAA-specified safety requirements, a runway can only be used if the tailwind and crosswind do not exceed the thresholds of 5 knots and 20 knots, respectively [9]. A wind state is defined as the set of wind vectors, *i.e.*, the set of wind strengths and wind directions, such that the same set of runways satisfies the corresponding threshold requirements. In other words, a wind state is defined by the runways that meet the threshold requirements and by the runways that do not. This approach follows the procedure developed by Li and Clarke [20]. Table 1 defines the 13 wind states at JFK. For instance, State 1 corresponds to a situation of calm winds, so that flights can be operated on all runways. In contrast, State 9 corresponds to the case of strong winds from the South, in which case runways $4L$, $4R$, $31L$ and $31R$ face above-threshold tailwinds.

Table 1: Definition of wind states at JFK: Set of runways that can be used per wind state

Wind States	1	2	3	4	5	6	7	8	9	10	11	12	13
$4L$, $4R$	✓	✓	✓	✓	✗	✓	✓	✗	✗	✓	✗	✗	✗
$22L$, $22R$	✓	✓	✓	✗	✓	✗	✗	✓	✓	✗	✓	✗	✗
$13L$, $13R$	✓	✓	✗	✓	✓	✓	✗	✓	✗	✗	✗	✓	✗
$31L$, $31R$	✓	✗	✓	✓	✓	✗	✓	✗	✓	✗	✗	✗	✓
Proportion	10.6%	7.6%	16.0%	8.9%	15.6%	2.5%	13.6%	8.1%	8.8%	10.3%	0.8%	0.5%	5.7%

2.3 Decision Variables

The decision in each period consists of two components:

- The runway configuration for the next period RC_t. This choice is constrained by the wind state: a runway configuration can only be used if each of its runways meets the threshold requirements. The set of runway configurations that can be selected when the wind state is ws_t is denoted by $\mathcal{RC}(ws_t)$. For each one of JFK's 8 main runway configurations, Table 2 indicates the set of wind states for which the configuration can be used. For instance, configuration $13L, 22L|13R$ can be used only in wind states that allow runways $13L$, $13R$ *and* $22L$ to be used, *i.e.*, in Wind States 1, 2, 5 and 8 (see Table 1). The selection of the runway configuration and the observation of the weather state determine, in turn, the Operational Throughput Envelope for the next period.

Table 2: Set of JFK runway configurations that can be selected per wind state

Wind States	1	2	3	4	5	6	7	8	9	10	11	12	13
$13L, 22L \vert 13R$	✓	✓	✗	✗	✓	✗	✗	✓	✗	✗	✗	✗	✗
$31L, 31R \vert 31L$	✓	✗	✓	✓	✓	✗	✓	✗	✓	✗	✗	✗	✓
$22L \vert 22R, 31L$	✓	✗	✓	✗	✓	✗	✗	✗	✓	✗	✗	✗	✗
$4R \vert 4L, 31L$	✓	✗	✓	✓	✗	✗	✓	✗	✗	✗	✗	✗	✗
$13L \vert 13R$	✓	✓	✗	✓	✓	✓	✗	✓	✗	✗	✗	✓	✗
$31R \vert 31L$	✓	✗	✓	✓	✓	✗	✓	✗	✓	✗	✗	✗	✓
$22L \vert 22R$	✓	✓	✓	✗	✓	✗	✗	✓	✓	✗	✓	✗	✗
$4R \vert 4L$	✓	✓	✓	✓	✗	✓	✓	✗	✗	✓	✗	✗	✗

- The rates at which arrivals and departures are served, respectively denoted by μ_t^a and μ_t^d. These service rates are controlled among the outermost set of achievable service rates for the selected runway configuration and the observed weather conditions. For instance, in Configuration 2 in Figure 1 and in VMC weather, the decision-maker can decide to operate with the arrival and departure service rates corresponding to point A or C or any other point on the VMC envelope. The decision-maker in fact selects the arrival service rate for the next period $\mu_t^a \in \{0, ..., A_{RC_t,wc_t}\}$. The upper bound of this choice A_{RC_t,wc_t} corresponds to the largest arrival throughput that can be realized in the selected runway configuration and observed weather conditions. In turn, the departure service rate μ_t^d is determined by the Operational Throughput Envelope corresponding to the selected runway configuration and the observed weather conditions. Hence, we can write: $\mu_t^d = \Phi_{RC_t,wc_t}(\mu_t^a)$, where Φ_{RC_t,wc_t} denotes the function that associates to the arrival service rate the value of the departure service rate when the airport operates in runway configuration RC_t and in weather conditions wc_t.

2.4 Dynamics of the System

2.4.1 Queue Dynamics

Arrival and departure queues are modeled by means of two dynamic and stochastic $M(t)/E_k(t)/1$ queuing models. The demand processes are modeled as Poisson processes, whose rates are determined by the number of landings and takeoffs scheduled per 15-minute period. The service processes are modeled as Erlang processes of order k, whose rates are controlled by the decision-maker. A value of $k = 3$ is used [17]. The model is non-stationary: the demand and service rates are time-varying. These rates are modeled as constant over any 15-minute period t and are thus denoted by λ_t and μ_t, respectively. Note that arrival and departure queues are not independent from each other since the arrival and departure service rates are subject to the same weather-related

constraints and jointly determined by the Operational Throughput Envelope. However, we assume that the stochastic evolution of the arrival queue is independent from that of the departure queue, *e.g.*, for given values of the arrival and departure service rates, the arrival queue might be longer than expected, while the departure queue might be shorter than expected.

This queuing model offers the advantage of being Markovian—and thus analytically tractable. Note, however, that it relies on specific assumptions on the demand and service processes. On the demand side, the use of the Poisson process has been challenged because of its memoryless property and alternative characterizations based on pre-scheduled flight times have been proposed [23]. On the service side, the analysis of surveillance data suggests that alternative characterizations (*e.g.*, a displaced exponential distribution) might provide a better fit of empirical inter-service times than the Erlang distribution, but the Erlang distribution was shown to also provide a reasonable approximation of the actual service process [29]. Moreover, the combination of the Poisson demand process and the Erlang service process into a dynamic $M(t)/E_k(t)/1$ queuing model has been shown to approximate well the magnitude and dynamics of airport queues observed in practice [22, 26, 17].

The state-transition diagram of the $M(t)/E_k(t)/1$ queuing system is shown in Figure 2. It relies on the characterization of an Erlang process of order k and rate μ as the succession of k independent and Markovian "stages of work" that are completed at rate $k\mu$. The state of the system is defined by the number of remaining stages of work, denoted by i. We introduce a time index s that varies continuously over the day and we denote by $P_i^S(s)$ the probability of being in state i at time s. Equation (1) shows the system of Chapman-Kolmogorov first-order differential equations describing the evolution of the state probabilities $P_i^S(s)$ over time period t, *i.e.*, between $(t-1)S$ and tS (where $S = 15$ min denotes the length of each period). The practical queue capacity is denoted by N. The system is assumed to be empty at the beginning of the day.

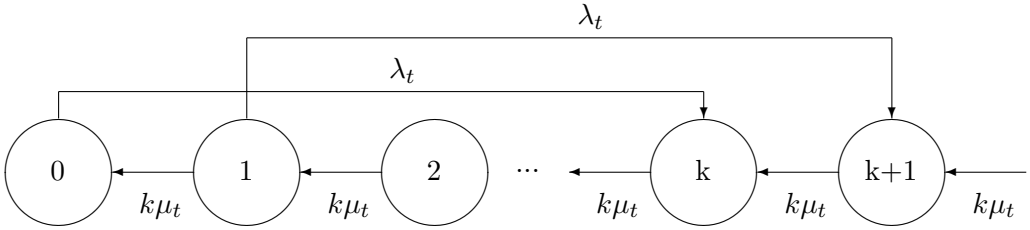

Figure 2: State-transition diagram of the $M(t)/E_k(t)/1$ queuing system

$$
\begin{array}{rcll}
\frac{dP_0^S(s)}{ds} & = & -\lambda_t P_0^S(s) + k\mu_t P_1^S(s) & \\
\frac{dP_i^S(s)}{ds} & = & -(\lambda_t + k\mu_t) P_i^S(s) + k\mu_t P_{i+1}^S(s) & \forall i \in \{1, ..., k\} \\
\frac{dP_i^S(s)}{ds} & = & \lambda_t P_{i-k}^S(s) - (\lambda_t + k\mu_t) P_i^S(s) + k\mu_t P_{i+1}(s) & \forall i \in \{k+1, ..., (N-1)k\} \\
\frac{dP_i^S(s)}{ds} & = & \lambda_t P_{i-k}^S(s) - k\mu_t P_i^S(s) + k\mu_t P_{i+1}^S(s) & \forall i \in \{(N-1)k+1, ..., kN-1\} \\
\frac{dP_{kN}^S(s)}{ds} & = & \lambda_t P_{k(N-1)}^S(s) - k\mu_t P_{kN}^S(s) &
\end{array}
\tag{1}
$$

Since decision-makers cannot observe the fine-grain state of the queues, *i.e.*, the number of remaining "stages of work", but observe the queue lengths instead, we proceed by aggregation. In other words, we map the state transition probabilities into queue length transition probabilities (Figure 3). This reduces the number of states of the arrival and departure queuing systems from $kN + 1$ to $N + 1$. In turn, this reduces the size of the state space of the DP model by a factor of k^2 and thus improves its tractability.

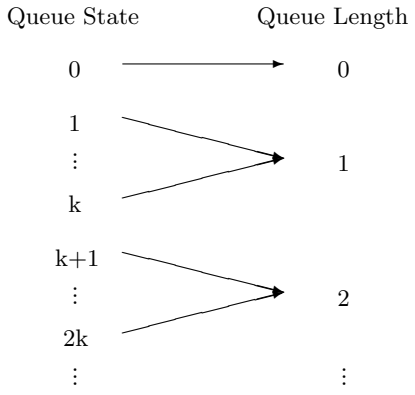

Figure 3: Mapping between queue states and queue lengths

In order to compute the queue length transition probabilities from the state transition probabilities, we assume that no aircraft is being served at the beginning of any period, *i.e.*, the system is in one of the states $\{mk, 0 \leq m \leq N\}$. The motivation for this choice is that the arrival and departure service rates are typically much greater than 1 per period. We denote the queue length transition probabilities over period t by $Q_{m,n}^t$, *i.e.*, if q_t denotes the queue length at the end of period t, then $Q_{m,n}^t = P(q_t = n | q_{t-1} = m)$. The probabilities $Q_{m,n}^t$ obviously depend on the demand and service rates λ_t and μ_t over period t and they are derived from the continuous state probabilities P^S according to the following relationship:

$$
\begin{array}{rcll}
Q_{m,0}^t & = & P_0^S(tS) & \\
Q_{m,n}^t & = & \sum_{l=1}^{k} P_{(n-1)k+l}^S(tS), & \forall n = 1, ..., N
\end{array}
\tag{2}
$$

where the state probabilities P^S are obtained by solving the system of differential equations (1), with the initial conditions:

$$P_i^S\big((t-1)S\big) = \begin{cases} 1, & \text{if } i = mk \\ 0, & \text{otherwise} \end{cases} \tag{3}$$

We solve the system (1) using the built-in differential equation solver ode45 in MATLAB 8.1. We store in a look-up table the queue length transition probabilities $Q^t_{m,n}$, for all m, n, λ_t, μ_t. In this way, we do not have to re-solve this system of equations at each iteration of the DP algorithm.

2.4.2 Runway Configuration Changes

A challenge in the development of any decision-making support tool to improve the control of runway configurations is to represent the costs of switching runway configurations. Switching configurations is, in fact, a challenging operational procedure that requires extensive coordination among several airport stakeholders, including airlines and air traffic controllers. Most importantly, queuing aircraft need to be re-routed, which may lead to operational inefficiencies and to the interruption of runway operations for some time. This creates a trade-off between potential operating enhancements resulting from configuration changes, on the one hand, and the costs of operating the configuration changes, on the other.

Several different ways to represent the costs associated with runway configuration changes have been used in the literature. The most straightforward way is to introduce a penalty cost c that is incurred each time a switch is implemented [20]. A second option is to introduce a time period of idleness during which the configuration switch is operated [5]. Finally, one could model configuration switches through reduced airport capacity (instead of zero capacity) during a longer period [32].

In this paper, we choose to represent this cost by a time period of idleness of the runway system, of length denoted by τ_I, during which arriving and departing aircraft may join the queue at an unchanged rate—determined by scheduling levels—but no flight is serviced. In other words, we assume that, if the decision-maker decides to change runway configurations at the beginning of the t^{th} period and chooses arrival and departure service rates $\mu^{(a)}$ and $\mu^{(d)}$ from the Operational Throughput Envelope of the new configuration, then the arrival and departure service rates are both equal to 0 during τ_I. After this, the arrival and departure service rates are, respectively, equal to $\mu^{(a)}$ and $\mu^{(d)}$ until the end of the 15-minute period. This situation is depicted in Figure 4.

Modeling runway configuration changes through a time period of idleness offers several advantages. First, it is a simple and transparent way to capture the trade-off between potential operating enhancements and the operating costs of configuration changes. If efficiency can be improved by changing configurations at a given time, this comes at the cost of temporary idleness and consequent initial build-up of the arrival and departure queues. The attractiveness of runway configuration

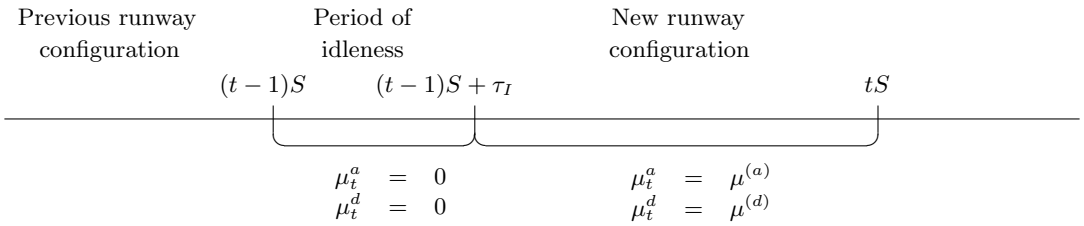

Figure 4: Schematic representation of a runway configuration change at the beginning of period t

changes depends on the duration of idleness τ_I. Second, it models the effects of configuration changes as increases in arrival and departure queue lengths and does not require the introduction of an artificial penalty cost c. Third, it enables the quantification of the sensitivity of optimal operating policies and arrival and departure queue lengths to the costs of configuration changes. Last, it can be efficiently integrated into our DP decision-making model, by modifying the queue length transition probabilities $Q^t_{m,n}$ (§ 2.4.1) to reflect the period of idleness following any configuration switch. Our DP framework, in fact, enables fine-grain calibration of the parameter τ_I, which can take any specified value—while previous approaches considered a duration of idleness equal to (or proportional to) the length of the decision-making period (*e.g.*, $S = 15$ min) [5].

Finally, this model of configuration changes enables the consideration of additional complexities at no computational cost. For instance, the duration of idleness resulting from a configuration change may vary as a function of the "proximity" of the two consecutive configurations [27]. Indeed, simply activating an additional runway for arrivals or departures (*e.g.*, activating Runway $4R$ when $4L$ is already in use) might be less disruptive than a move to a very different configuration that requires a change in the entire flow of arriving and departing aircraft. For this reason, we denote by $\tau_I^{RC_1,RC_2}$ the duration of idleness following the change from runway configuration RC_1 to runway configuration RC_2.

Note that, in practice, the operational cost of configuration changes might also depend on other system characteristics. For instance, it might increase with the extent of congestion at the time of the change, *i.e.*, with the number of arriving and departing queuing aircraft. As well, it might be larger under IMC than under VMC. These additional complexities can also be captured in our model at no computational cost by making the duration of the idleness τ_I a function of additional state components, *e.g.*, a_{t-1}, d_{t-1} and wc_t. The framework presented in this paper could also be extended to capture alternative characterizations of the operating costs of runway configuration changes, *e.g.*, with a marginally decreasing impact on capacity [32].

2.4.3 Weather and Wind Dynamics

Weather and wind dynamics are modeled by means of Markov chains. Weather variations are modeled as a time-varying two-state Markov chain. We denote by p_t (resp. q_t) the transition

probability from state VMC to state IMC (resp. from IMC to VMC) over period t. The time-dependence of p_t and q_t is intended to capture potential variations in weather dynamics over the course of the day and to incorporate weather forecasts. The transition matrix of the weather Markov chain, denoted by P_t^{wc}, is given by:

$$P_t^{wc} = \begin{array}{c} \\ VMC \\ IMC \end{array} \begin{array}{c} \begin{array}{cc} VMC & IMC \end{array} \\ \begin{pmatrix} 1-p_t & p_t \\ q_t & 1-q_t \end{pmatrix} \end{array}$$

Note that additional weather states could be considered [21]. This would enable more fine-grain characterization of the weather dynamics at the airport. However, this would increase the complexity of the decision-making problem. Moreover, it would make the corresponding estimates of the Operational Throughput Envelopes of the different runway configurations (see Figure 1) less statistically reliable as each would be based on a smaller data sample. We therefore restrict our attention to this two-state model.

A similar Markov chain is introduced to characterize the wind dynamics. It is defined by the transition probability from State i to State j, for all pairs of wind states (i, j) (see Table 1).

We describe how the transition probabilities of these two Markov chains are estimated in § 3.1.

2.5 Cost Function

The control strategy aims to minimize congestion costs, which are typically modeled as a non-decreasing function of the queue length with non-decreasing marginal costs. In this paper, we consider a quadratic cost function of the arrival and departure queue lengths, since the expected total delay scales quadratically with the number of queuing aircraft. Moreover, the costs associated with arrival queues are weighted by a factor $\alpha \geq 1$. This is to capture the fact that arrival delays and departure delays may have different costs, as arriving aircraft can be more challenging and expensive to hold in queue than departing aircraft.

The cost function is written as follows:

$$\alpha \sum_{t=1}^{T} a_t^2 + \sum_{t=1}^{T} d_t^2. \tag{4}$$

2.6 Dynamic Programming Formulation

As described in § 2.3, we denote by $\mathcal{RC}(ws)$ the set of runway configurations that can be selected in wind state ws and by $A_{RC,wc}$ the maximal arrival rate that can be handled in runway configuration RC and in weather conditions $wc \in \{VMC, IMC\}$. We denote the cost-to-go function by $J_t(a_{t-1}, d_{t-1}, RC_{t-1}, wc_t, ws_t)$, which represents the expected total cost of being in state $(a_{t-1}, d_{t-1}, RC_{t-1}, wc_t, ws_t)$ at the beginning of period t. The decision-maker minimizes the sum

of the expected congestion costs experienced at the end of period t (*i.e.*, $\alpha E\left[a_t^2\right] + E\left[d_t^2\right]$) and the future congestion costs from period $t+1$ onward (*i.e.*, $E\left[J_{t+1}\left(a_t, d_t, RC_t, wc_{t+1}, ws_{t+1}\right)\right]$). The Bellman equation is written as follows:

$$J_t(a_{t-1}, d_{t-1}, RC_{t-1}, wc_t, ws_t) = \min_{\substack{RC_t \in \mathcal{RC}(ws_t) \\ \mu_t^a \in \left[0, A_{RC_t, wc_t}\right]}} \Big(\alpha E\left[a_t^2\right] + E\left[d_t^2\right] + E\left[J_{t+1}\left(a_t, d_t, RC_t, wc_{t+1}, ws_{t+1}\right)\right] \Big), \forall t = 1, ..., T \quad (5)$$

$$J_{T+1}(a_T, d_T, RC_T, wc_{T+1}, ws_{T+1}) = 0 \quad (6)$$

The arrival queue a_t at the end of period t depends on the number of scheduled arrivals x_t during period t, on the duration of idleness $\tau_I^{RC_{t-1}, RC_t}$, if any, on the arrival rate μ_t^a during period t and on the previous period's arrival queue length a_{t-1}. Similarly, the departure queue d_t depends on the variables y_t, $\tau_I^{RC_{t-1}, RC_t}$, μ_t^d and d_{t-1}. A summary of the dependencies described in § 2.4 is provided below—solid lines denote system evolution and dashed lines denote constraints on the decisions.

$$\begin{aligned} ws_t &\dashrightarrow RC_t \\ RC_{t-1}, RC_t &\longrightarrow \tau_I^{RC_{t-1}, RC_t} \\ RC_t, wc_t &\dashrightarrow \mu_t^a, \mu_t^d = \Phi_{RC_t, wc_t}\left(\mu_t^a\right) \\ x_t, \tau_I^{RC_{t-1}, RC_t}, wc_t, \mu_t^a, a_{t-1} &\longrightarrow a_t \\ y_t, \tau_I^{RC_{t-1}, RC_t}, wc_t, \mu_t^d, d_{t-1} &\longrightarrow d_t \end{aligned}$$

3 Solution Algorithm

3.1 Experimental Setup

We apply the model at JFK Airport. We consider the schedule of flights on the 9 days which correspond to the 9 deciles of the distribution of the number of daily flights at JFK in 2007. These days capture the variability of flight schedules over the year. Unless otherwise specified, we present results obtained with the schedule of flights on 05/25/2007, which corresponds to the 9^{th} decile of this distribution. The schedule of landings and takeoffs for each day is obtained from the Aviation Performance Metrics (APM) database [10]. Figure 5 shows the schedule at JFK on 05/25/2007. Note that the proportion of arrivals and departures varies over the course of the day: significantly more departures than arrivals are scheduled in the morning, while the reverse is true in early afternoon.

We categorize the 8 major runway configurations at JFK into 4 sets of two configurations each:

- Configurations with two arrival runways and one departure runway: $13L, 22L|13R$ and $31L, 31R|31L$. They can achieve the largest arrival rates.

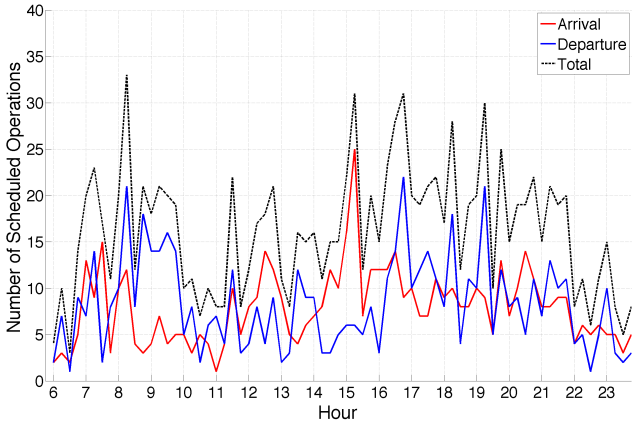

Figure 5: Arrival and departure schedules at JFK on 05/25/2007

- Configurations with one arrival runway and two departure runways: $22L|22R, 31L$ and $4R|4L, 31L$. They achieve the largest departure rates when few landings are operated.
- Configurations with two independent parallel runways: $13L|13R$ and $31R|31L$. They achieve a larger departure rate than configurations with two arrival runways and one departure runway when few landings are operated, since departures are less constrained by aircraft landing and taxiing in. However, they achieve a lower throughput than configurations with two arrival runways and one departure runway when a large number of landings are operated.
- Configurations with two more closely spaced runways: $22L|22R$ and $4R|4L$. They achieve the lowest service rates. This is mainly due to the location of the runways relative to the terminal complex, since aircraft taxiing in have to cross the departure runway.

The Operational Throughput Envelopes of these runway configurations are obtained from Simaiakis [28] and shown in Figure 6. For each of the 4 sets described above, we plot the envelope of the configuration that achieves the largest service rates with a solid line and, in the same color, the envelope of the other configuration in the same set with a dashed line. In addition, each dot represents the number of scheduled landings and takeoffs per 15-minute period on 05/25/2007. Note that the scheduling levels exceed airport capacity during a large number of periods even in VMC (Figure 6a). These imbalances are even larger in IMC (Figure 6b). This is likely to lead to significant flight delays. Note, moreover, that the relative capacity of the different configurations is similar under VMC and IMC. For instance, the configurations that achieve the largest departure throughput under VMC also achieve the largest departure throughput under IMC.

We calibrate our Markovian weather model as follows. We, first, compute the optimal policy assuming that the airport operates in VMC throughout the day, *i.e.*, we set the weather transition probabilities equal to $p_t = 0$ and $q_t = 1$ for all periods t. Note that, by doing so, we do derive the

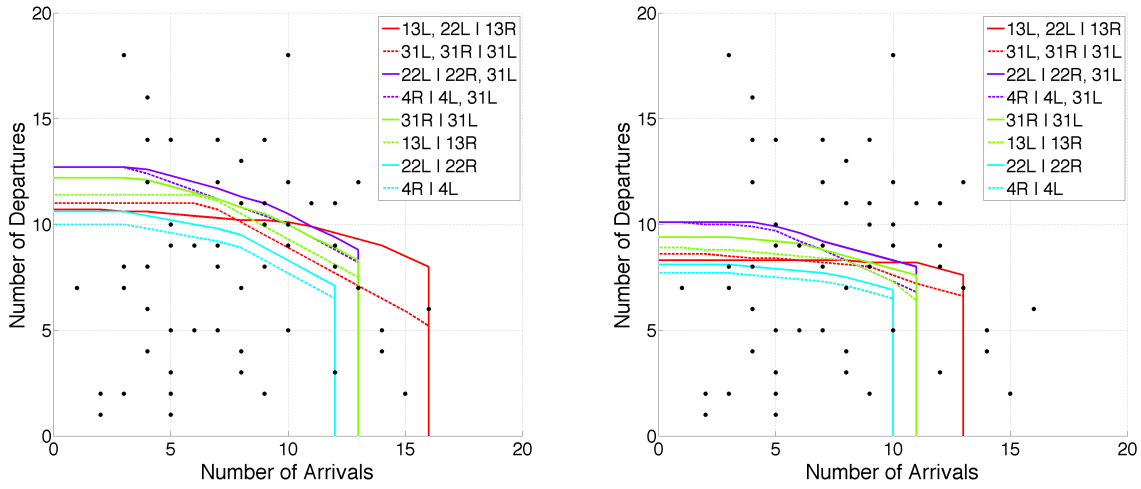

(a) VMC Envelopes

(b) IMC Envelopes

Figure 6: Operational Throughput Envelopes of the main runway configurations at JFK [28]

optimal policy if the system is in State IMC at any period t, but this decision is made under the assumption that the airport will operate in VMC from period $t+1$ to period T. We then update the policies if a weather forecast predicts that the airport will operate under IMC at some periods of the day. This procedure is detailed in § 3.3 and tested in § 3.4.

Wind transition probabilities are estimated by their maximum likelihood estimator using historical records of operations [10]. In other words, we estimate the transition probability from State i to State j by the ratio $\frac{n_{ij}}{n_i}$, where n_{ij} (resp. n_i) designates the number of transitions from State i to State j (resp. the number of periods in State i). This follows the procedure developed by Li and Clarke [20]. Note that the model can easily be extended to incorporate wind forecasts.

Unless otherwise specified, we use the same duration of idleness $\tau_I^{RC_1,RC_2}$ for all pairs of runway configurations $RC_1 \neq RC_2$. To simplify notation, we denote it by τ_I in the remainder of the paper. This assumption can be easily modified to introduce differing values of this parameter for different configuration pairs. We provide an example in § 4.1. The purpose of our experimental tests is to capture the trade-off between potential operating enhancements and the operating costs of configuration changes, for different values of τ_I—as described in § 2.4.2. Sensitivity analyses will quantify the impact of τ_I on optimal policies and expected queue lengths. In practice, the parameters τ_I can be calibrated by airport operators on a case-by-case basis. As previously mentioned, additional complexities (*e.g.*, dependencies on the extent of congestion, on weather conditions, etc.) can be easily integrated into the decision-making model.

We consider a value of $\alpha = 1$, *i.e.*, we assume that arrival and departure delays have identical costs. We investigate the sensitivity of optimal policies and expected queue lengths to α in § 4.3.

Finally, we set the value of the practical queue capacity at $N = 30$. Note that a small value of N may lead to underestimation of the expected arrival and departure queues. On the other hand, a large N will increase computational times, as the number of states scales quadratically with N. We have, in fact, tested a JFK scenario with a larger value of $N = 40$, which implies an almost 75 percent increase in the number of queuing system states from 961 ($=31^2$) to 1681 ($=41^2$) and, consequently, greatly increases computational times. Only marginal differences were observed in the optimal policies, compared to $N = 30$. A capacity of $N = 30$ for (each of) the arrival queue and the departure queue therefore appears to be sufficiently large to minimize the effects of the finite queue size for the JFK application.

3.2 Exact Dynamic Programming Algorithm

First, an exact DP algorithm is implemented using the solution concept of backward induction [2, 3]. The optimal policy in the final period (*i.e.*, between 23:45 and 24:00) is computed for all possible states, *i.e.*, for all possible arrival and departure queue lengths that can be observed at 23:45, for all possible runway configurations that can be used in the previous period (*i.e.*, between 23:30 and 23:45) and for all possible weather and wind conditions. This provides optimal costs in the final period as a function of the state of the system at the beginning of the final period. This cost is then used to compute optimal policies in the second-to-last period, as a function of the state of the system at 23:30. This process is repeated until the optimal policies for all periods have been derived.

The exact DP algorithm is executed in approximately 90 minutes on a laptop computer. The optimal policy for the entire day of operations can thus be easily obtained off-line, *i.e.*, before the beginning of the day. This policy is based on the original model parameters, including the original schedule of flights and the original weather forecast (*e.g.*, assuming that the airport will operate under VMC).

However, the policy determined off-line might no longer be optimal in the face of dynamic disturbances that may occur during the day of operations. For instance, the airport might be subject to schedule updates (*e.g.*, upstream delays, en-route congestion, the initiation of Ground Delay Programs, surface congestion, etc.) or changes in weather forecasts. In these instances, the policy might need to be dynamically revised over the course of the day using real-time information. But given its computational requirements, the exact DP algorithm is likely to exceed the time frame of actual decision-making by air traffic controllers. For this reason, we implement an approximate algorithm, described below, to perform the dynamic revisions. This greatly accelerates execution and consequently enables the policies to be updated in real time.

3.3 One-Step Look-Ahead Algorithm

In this section, we develop an approximate solution algorithm based on a one-step look-ahead. The solution architecture is shown in Figure 7. In the upper part, we consider the policy obtained off-line with the exact DP algorithm (§ 3.2), based on the original model parameters (*e.g.*, the original schedule of flights and the original weather forecast). We denote this policy by $\left(\widehat{RC}_t, \widehat{\mu_t^a}\right)$ and its associated expected cost-to-go function by $\widehat{J}$.

In the lower part, we consider an operational disturbance (*e.g.*, a schedule update, a new weather forecast, etc.) which leads to a change in the model's inputs and parameters (*e.g.*, x_t, y_t, p_t, q_t). Ideally, one would apply the exact DP algorithm with the updated model parameters. This would yield the optimal revised policy, which we denote by $\left(\overline{RC}_t, \overline{\mu_t^a}\right)$.

However, the computational times of the exact DP algorithm prevents this policy from being obtainable in real time. We therefore derive a revised policy with a one-step look-ahead algorithm based on the cost-to-go function $\widehat{J}$. In other words, we choose, at the beginning of period t, the policy that minimizes expected total costs, assuming that costs from period $t+1$ onward are given by $\widehat{J}$. The policy for period t, denoted by $\left(\widetilde{RC}_t, \widetilde{\mu_t^a}\right)$, is determined as follows [4]:

$$\left(\widetilde{RC}_t, \widetilde{\mu_t^a}\right) \quad = \quad \underset{\substack{RC_t \in \mathcal{RC}(ws_t) \\ \mu_t^a \in \left[0, A_{RC_t, wc_t}\right]}}{\arg\min} \left(\alpha E\left[a_t^2\right] \; + \; E\left[d_t^2\right] \; + \; E\left[\widehat{J}_{t+1}\left(a_t, d_t, RC_t, wc_{t+1}, ws_{t+1}\right)\right] \right) \quad (7)$$

The execution of this algorithm is almost instantaneous and thus well suited to the actual problem faced by air traffic controllers. In turn, this fast approximation scheme can be implemented in real time when new information becomes available. The performance of this approach depends on how well the look-ahead policy, $\left(\widetilde{RC}_t, \widetilde{\mu_t^a}\right)$, approximates the optimal revised policy, $\left(\overline{RC}_t, \overline{\mu_t^a}\right)$. We evaluate this performance in the next section.

3.4 Evaluation of Performance

In order to test the performance of our approach, we first simulate schedule disturbances and we then simulate weather forecasts. We can simulate wind forecasts similarly. In each instance, we compare the expected congestion costs resulting from the application of (a) the optimal policy with the updated model parameters, $\left(\overline{RC}_t, \overline{\mu_t^a}\right)$, which might be too computationally time-consuming to be determined in real time, (b) the optimal policy with the original model parameters, $\left(\widehat{RC}_t, \widehat{\mu_t^a}\right)$, and (c) the approximate policy produced by the one-step look-ahead algorithm with the updated model parameters (Equation (7)), $\left(\widetilde{RC}_t, \widetilde{\mu_t^a}\right)$. We report the average error of policies $\left(\widehat{RC}_t, \widehat{\mu_t^a}\right)$ and $\left(\widetilde{RC}_t, \widetilde{\mu_t^a}\right)$, defined as the relative increase in congestion costs as compared to policy $\left(\overline{RC}_t, \overline{\mu_t^a}\right)$.

The purpose of this comparison is to show that we obtain close-to-optimal policies under various demand and weather scenarios that might arise in practice at the airports. Note that the

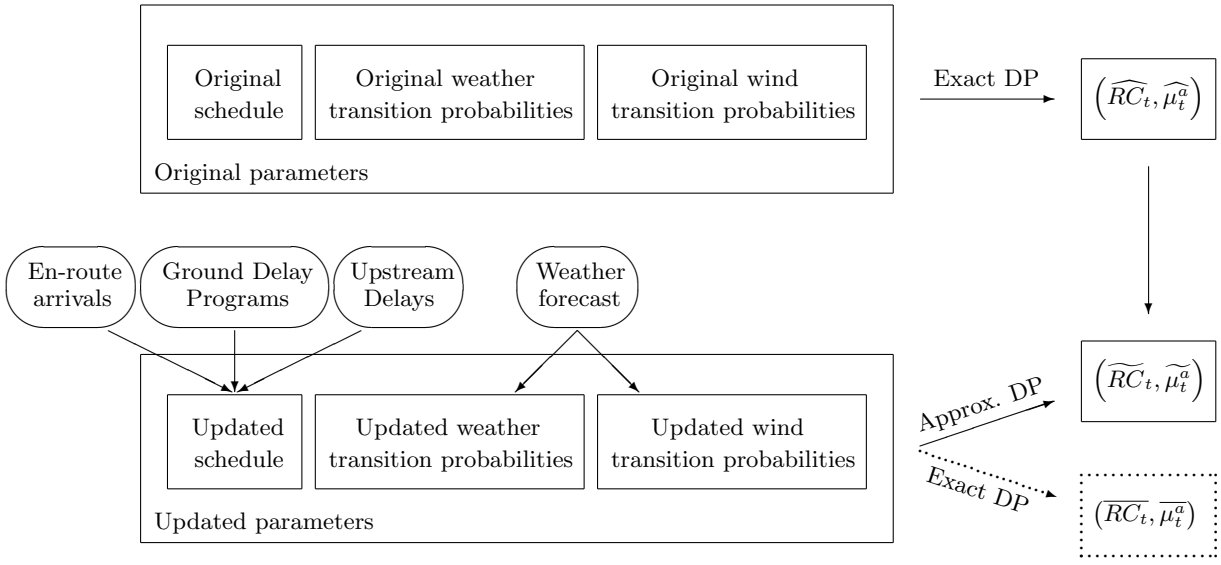

Figure 7: Representation of the solution architecture

goal here is *not* to develop an accurate model of schedule disturbances or weather variations. Instead, we simulate realistic examples of such disturbances and we evaluate the performance of the approximation scheme developed in § 3.3.

We simulate a schedule disturbance as follows: at each period, we introduce a schedule perturbation randomly sampled from the integers within ε of the original number of scheduled arrivals and departures. For instance, if 10 arrivals and 15 departures are originally scheduled during a given period, then we uniformly sample, for a value of $\varepsilon = 20\%$, the updated number of arrivals (resp. departures) from the five integers between 8 and 12 (resp. from the seven integers between 12 and 18). Note that the expected total number of flights in the updated schedule is identical to that of the original schedule. For each value of ε considered, we simulate 10 schedules of flights according to this procedure and we report in Table 3 the average relative error of each policy.

First, note that the optimal policy computed off-line with the original schedule, $\left(\widehat{RC}_t, \widehat{\mu}_t^a\right)$, performs reasonably well, even after schedule updates. Even for the largest schedule perturbations, this policy still results in expected congestion costs within 5% to 10% of the optimal congestion costs. Moreover, the one-step look-ahead algorithm significantly improves the performance over the original policy. Indeed, policy $\left(\widetilde{RC}_t, \widetilde{\mu}_t^a\right)$ results in expected congestion costs that exceed optimal costs by only 1% to 2%, for different levels of schedule perturbations. In addition, results suggest that the look-ahead algorithm performs consistently well for different schedule updates. For instance, for the 20 simulated schedules corresponding to $\varepsilon = 40\%$ and $\varepsilon = 50\%$, the error of policy $\left(\widetilde{RC}_t, \widetilde{\mu}_t^a\right)$ ranges from 0.63% to 2.76%.

We proceed similarly to test the performance of the policies $\left(\widehat{RC}_t, \widehat{\mu}_t^a\right)$ and $\left(\widetilde{RC}_t, \widetilde{\mu}_t^a\right)$ in the case of a change in the weather forecast. As described in § 3.1, the original policy $\left(\overline{RC}_t, \overline{\mu}_t^a\right)$ was

Table 3: Total expected congestion costs with the three policies under a schedule update, for different values of ε

	Optimal Policy	Available Policies	
	$\left(\overline{RC}_t, \overline{\mu}_t^a\right)$	$\left(\widehat{RC}_t, \widehat{\mu}_t^a\right)$	$\left(\widetilde{RC}_t, \widetilde{\mu}_t^a\right)$
Schedule Considered	Updated	Original	Updated
Algorithm	Exact	Exact	Look-Ahead
Available on-line?	No	Yes	Yes
$\varepsilon = 10\%$	Baseline	+0.44%	+0.12%
$\varepsilon = 20\%$	Baseline	+1.33%	+0.38%
$\varepsilon = 30\%$	Baseline	+2.70%	+0.82%
$\varepsilon = 40\%$	Baseline	+4.09%	+1.16%
$\varepsilon = 50\%$	Baseline	+6.45%	+1.96%

obtained for an "all-VMC" day, *i.e.*, with weather transition probabilities equal to $p_t = 0$ and $q_t = 1$ for all periods t. We now introduce weather variations. First, we simulate 20 deterministic weather scenarios for the entire day of operations and define the corresponding values of p_t and q_t—note that, in the case of a deterministic forecast, p_t and q_t take only the values 0 and 1. Then, we simulate 20 deterministic weather forecasts for half the day of operations (*i.e.*, between 6 a.m. and 3 p.m.). We set the corresponding values of p_t and q_t for the half-day—again, equal to 0 or 1. For the remainder of the day (*i.e.*, between 3 p.m. and midnight), we estimate the values of p_t and q_t by their maximum likelihood estimator using historical records of operations, *i.e.* $p_t = 0.0440$ and $q_t = 0.0557$ [17]. This aims to capture situations where weather forecasts are available for a limited time only and later forecasts exhibit uncertainty. In both cases, we add a 21^{st} scenario corresponding to an "all-IMC" day (or half-day). This represents the largest weather forecast error.

Since expected arrival and departure queue lengths are larger under deteriorated weather, the practical queue capacity $N = 30$ might be insufficient for an "all-IMC" day with very heavy traffic. We therefore consider, for this particular set of tests, the schedule of flights on 09/18/2007, which corresponds to the median of the distribution of the number of daily flights at JFK in 2007. We sort the two sets of 20 weather forecasts by increasing error of the look-ahead algorithm and report the results in Figure 8.

Note, first and foremost, that the error of the two available policies, *i.e.*, $\left(\widehat{RC}_t, \widehat{\mu}_t^a\right)$ and $\left(\widetilde{RC}_t, \widetilde{\mu}_t^a\right)$ is extremely small. The error of the original policy $\left(\widehat{RC}_t, \widehat{\mu}_t^a\right)$ is within 1% to 3% under all weather scenarios. Again, the one-step look-ahead algorithm results in a significant performance improvement and the cost of the updated policy $\left(\widetilde{RC}_t, \widetilde{\mu}_t^a\right)$ is within 2% of the optimal congestion costs in all scenarios considered. Moreover, the error of the two policies seems much smaller in this case than in the case of a schedule update. This might be explained by the fact that

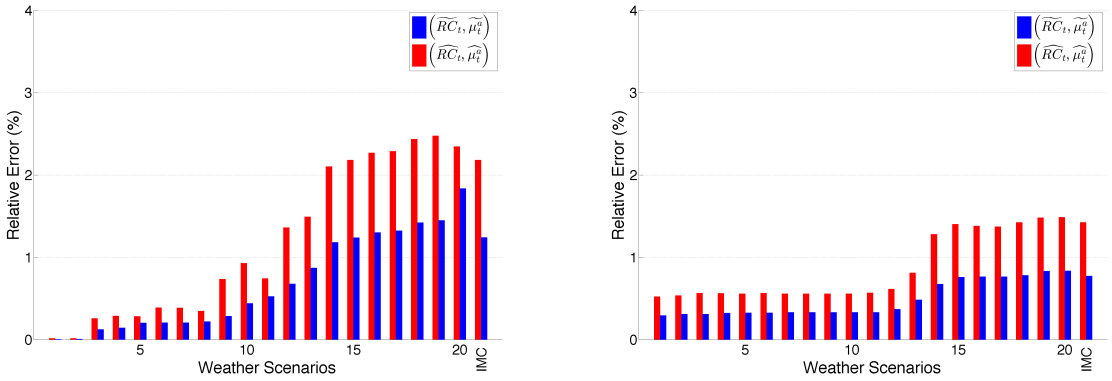

(a) Full-day forecasts

(b) Half-day forecasts

Figure 8: Total expected congestion costs with the three policies, under different weather scenarios

the VMC and IMC Operational Throughput Envelopes (Figure 6) are relatively similar to each other, so optimal policies are similar in VMC and IMC. Finally, note that the "all-IMC" scenario does not yield the largest error, which might suggest that *changes* in weather conditions might cause larger policy updates than *errors* in weather forecasts.

In conclusion, the solution architecture shown in Figure 7, combining an exact DP algorithm and one-step look-ahead algorithm provides a fast and accurate approximation of optimal policies. It therefore provides a flexible on-line decision-making tool to help minimize congestion costs by dynamically controlling runway configurations and arrival and departure service rates using real-time information on flight schedules and meteorological conditions.

4 Computational Results

In this section we present the results of the application of the exact DP algorithm to JFK. § 4.1 characterizes the optimal policies. § 4.2 shows the frequency of use of different runway configurations and of arrival/departure balances over the course of the day when the optimal policy is applied. § 4.3 discusses the sensitivity of expected queue lengths to several model parameters. In order to isolate the effects of the schedule of flights and of queue stochasticity on optimal policies and queue lengths, we restrict the presentation of our computational results to an all-VMC day (*i.e.*, $p_t = 0$ and $q_t = 1$, $\forall t$), but similar results are obtained when different weather forecasts are considered. All results shown are obtained with the schedule on 05/25/2007, unless otherwise specified.

4.1 Optimal Policies

The optimal policy derived from the exact DP algorithm is a function that determines the runway configuration and the arrival and departure service rates at each period of the day and in any state

of the system. Figure 9 plots the contours of the optimal arrival rate μ_t^a and the optimal runway configuration RC_t for the period t that begins at 12:00, for a value of $\tau_I = 5$ minutes, when the airport operates in Wind State 1 (*i.e.*, all runway configurations can be used), as a function of the arrival and departure queue lengths that are observed at the beginning of the period (*i.e.*, at 12:00). Note that the departure rate is not shown explicitly in the figure, but it is uniquely determined through the VMC Operational Throughput Envelope of the selected runway configuration. During the period considered, 8 landings and 4 takeoffs were scheduled, and, more generally, more arrivals than departures were scheduled between 11:45 and 13:00 (see Figure 5). Two cases are considered: Figure 9a (resp. Figure 9b) shows the optimal policy at 12:00 when the airport operated in the previous period (*i.e.*, between 11:45 and 12:00) in runway configuration $13L, 22L|13R$ (resp. in runway configuration $22L|22R, 31L$).

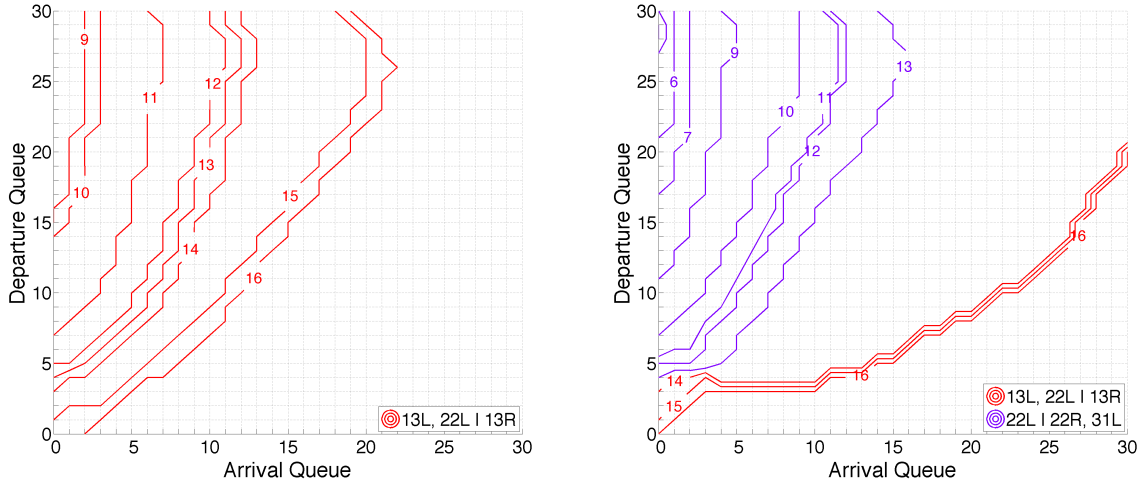

(a) $RC_{t-1} = 13L, 22L|13R$ (b) $RC_{t-1} = 22L|22R, 31L$

Figure 9: Optimal runway configuration and arrival rate at 12:00 ($\tau_I = 5$ min, $ws_t = 1$)

Several observations can be made about the optimal policy. First, the optimal arrival rate is non-decreasing as a function of the arrival queue length and non-increasing as a function of the departure queue length, with the exception of some "boundary effects" when queue lengths approach the practical queue capacity N. In other words, the longer the arrival queue, the more available capacity should be allocated to arriving aircraft. Moreover, the optimal policy depends on the runway configuration in use. For example, when the airport operates in configuration $13L, 22L|13R$, the optimal policy is to stay in this configuration, which allocates two runways to arrivals and one runway to departures, in order to serve a larger number of arriving aircraft during the considered period (Figure 9a). In contrast, if the airport operates in configuration $22L|22R, 31L$, which allocates two runways to departures and one runway to arrivals, it may be optimal to switch

to configuration $13L, 22L|13R$ if the departure queue is small enough or, equivalently, if the arrival queue is large enough, or to stay in configuration $22L|22R, 31L$ otherwise (Figure 9b). In addition, whereas the selected arrival rate increases quite smoothly as a function of the arrival queue length in the case where $RC_{t-1} = 13L, 22L|13R$ (Figure 9a), it increases discontinuously from 13 to 16 when $RC_{t-1} = 22L|22R, 31L$ (Figure 9b).

In order to illustrate these points, let us consider the evolution of the optimal arrival rate as a function of the arrival queue observed at the beginning of period t, when the departure queue length is equal to 10 aircraft. If configuration $13L, 22L|13R$ was in use in period $t-1$ (Figure 9a), then the decision-maker operates in the same configuration in period t. The longer the arrival queue observed at the beginning of the period, the larger the selected arrival rate. When 12 or more arriving aircraft are queuing, then the decision-maker selects the largest arrival rate available (16 in this case). In contrast, if configuration $22L|22R, 31L$ was in use in period $t-1$ (Figure 9b), then the decision-maker stays in configuration $22L|22R, 31L$ if the arrival queue length is sufficiently small. The optimal arrival service rate increases quite smoothly from 9 when no arriving aircraft are queuing to 13 when 7 arriving aircraft are queuing. As the arrival queue length increases from 7 to 21, the optimal policy remains invariant: the decision-maker selects the largest arrival rate that can be achieved under the runway configuration in use (13 in this case). If, however, 22 or more arriving aircraft are queuing, then the decision-maker switches to configuration $13L, 22L|13R$ in order to increase the arrival rate (to 16 in this case). In other words, when the arrival queue exceeds a certain threshold, then it might become beneficial to switch to another configuration that enhances the arrival throughput, in this case to configuration $13L, 22L|13R$, if the operational benefits associated with the switch become large enough to offset the costs associated with the time period of idleness following the runway configuration change.

4.2 Frequency of Decisions

In this section, we compute the state probabilities of the system over the day when the optimal policy is applied and we report the frequency of decisions at each period. Figure 10 shows the frequency of use for each of the four sets of runway configurations defined in § 3.1 at each period of the day, for different values of τ_I. As expected, the frequency of use for these different configurations depends on the throughput they achieve (Figure 6). Since the three-runway configurations achieve the largest service rates, they are the most frequently used ones. In contrast, the two-runway configurations are mostly used in adverse wind conditions when the airport can only operate on a small subset of runways. Configurations including the two widely-spaced parallel runways, 13/31, are used more frequently than configurations with the two more closely-spaced parallel runways, 4/22, because of the significant difference in the capacity of the corresponding configurations.

Moreover, the exact timing of use of the different configurations depends on the arrival and departure schedules, as well as the evolution of the operations through the day. Importantly, note

that no runway configuration is used 100% of the time at any period of the day. This indicates that the stochasticity of the system has an impact on the optimal control, as suggested by Figure 9. Finally, the use of different runway configurations depends on the value of the parameter τ_I. Indeed, in the case where $\tau_I = 0$ min, runway configuration changes are very frequent to make the best possible use of available capacity. For larger values of τ_I, however, the cost associated with the idleness of the runway system is more likely to exceed the operational benefits associated with switching from one configuration to another and consequently runway configuration changes become less frequent. For instance, if $\tau_I = 0$, the decision-maker should operate, whenever possible, in a configuration with two departure runways between 13:00 and 14:00 to best serve the departure peak at that time (see Figure 5). As τ_I increases, decisions trade off congestion costs with increasing switching costs, depending on the observed number of queuing aircraft on the ground and in the air. As a result, the frequency of a switch between 13:00 and 14:00 becomes smaller. When $\tau_I = 10$ min, then it is almost always optimal to stay in a configuration with two arrival runways and one departure runway for the entire period between 11:00 and 17:00.

As mentioned in § 2.4.2, the modeling framework developed in this paper enables us to introduce differentiated costs of runway configuration changes as a function of the proximity of configurations. We compare in Figure 11 the use of runway configurations when the duration of idleness following a runway configuration change, τ_I, is uniform across runway configuration changes (Figure 11a) to the case where the values of τ_I vary with the runway configuration change considered (Figure 11b). Specifically, we assume in Figure 11b values of τ_I equal to (a) 1 minute if the switch merely disturbs operations by simply adding or removing a third runway (*e.g.*, when switching between $31L, 31R|31L$ and $31R|31L$), (b) 5 minutes if the switch involves a 90-degree reorientation of the flow of aircraft (*e.g.*, from $22L|22R, 31L$ to $31R|31L$) and (c) 10 minutes if the switch involves a 180-degree reorientation of the flow of aircraft (*e.g.*, from $31L, 31R|31L$ to $13L|13R$). In contrast, we assume in Figure 11a a single value of τ_I equal to 3 minutes, which is approximately the average value of τ_I in the differentiated case. Any differences between Figures 11a and 11b can thus be attributed essentially to the differences in the *distribution* of τ_I across configuration changes.

As expected, differentiated costs of configuration changes can impact significantly the optimal policies. For instance, it may be optimal to switch from a configuration with two arrival runways and one departure runway at 13:00 to a configuration that enables the selection of a larger departure rate in order to best serve the large number of takeoffs between 13:00 and 14:00. Even though the departure throughput could be maximized by using a configuration with two departure runways, it may be optimal to operate during this period in a configuration with two independent parallel runways (*i.e.*, $13L|13R$ or $31R|31L$). This is because the costs of switching from configuration $13L, 22L|13R$ to $13L|13R$ or from $31L, 31R|31L$ to $31R|31L$ may be lower than the costs of switching to $22L|22R, 31L$ or to $4R|4L, 31L$. In this case, it may be optimal to increase moderately the departure throughput by using a "closer" configuration than to increase the departure throughput

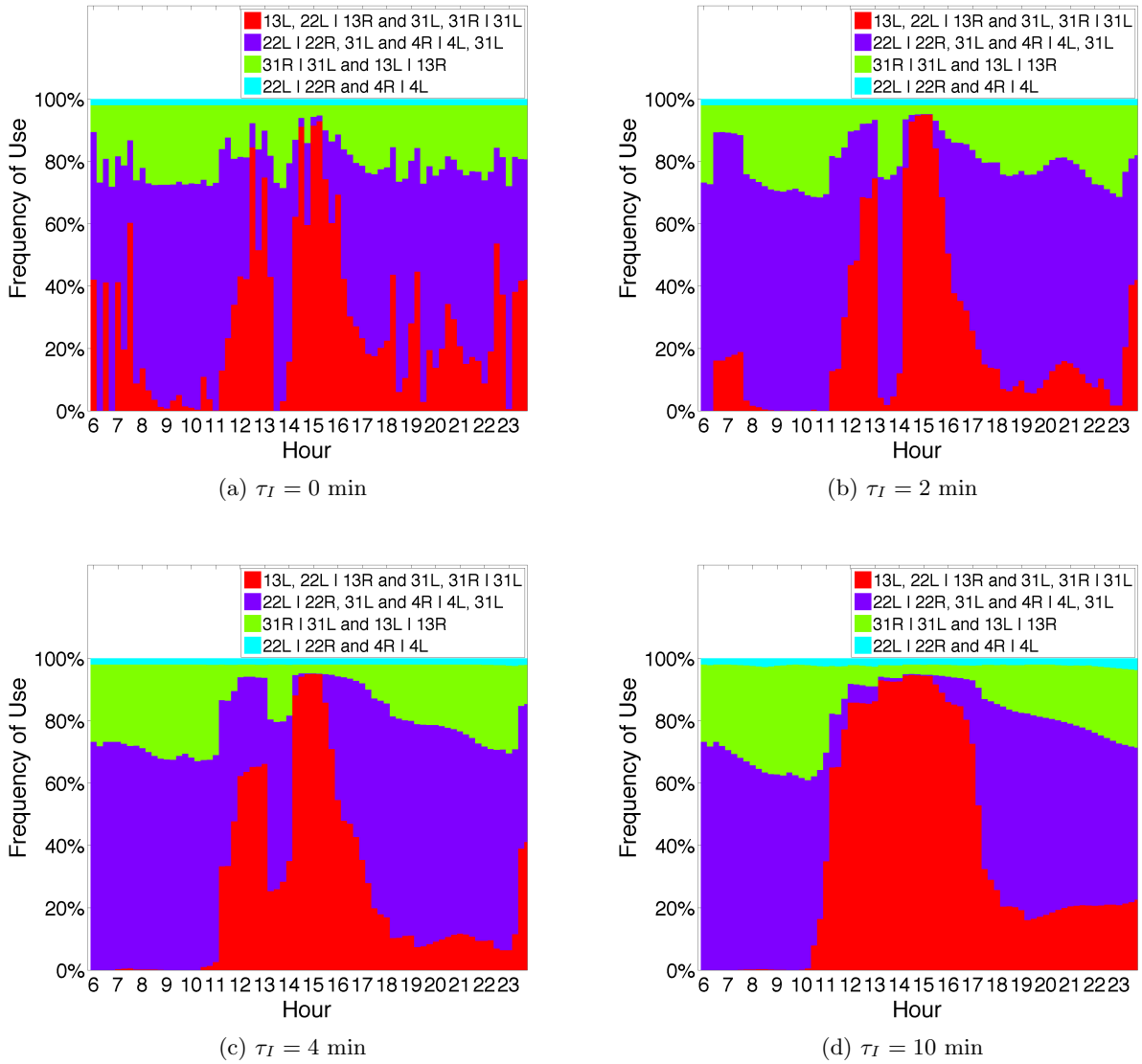

(a) $\tau_I = 0$ min

(b) $\tau_I = 2$ min

(c) $\tau_I = 4$ min

(d) $\tau_I = 10$ min

Figure 10: Frequency of use of each runway configuration for different values of τ_I

to a greater extent at a larger operational cost. In turn, the distribution of τ_I across configuration changes can affect congestion costs. We estimate that the application of the optimal policy obtained with the same value of τ_I for all configuration changes in the case where the values of τ_I vary with configuration changes leads to an increase in total expected congestion costs by 5.19%, as compared to the application of the optimal policy obtained with differentiated values of τ_I. Results from these tests suggest that the fine-grain and flexible calibration by airport operators of the operational costs associated with runway configuration changes enabled by our DP model can result in significant improvements in the efficiency of operating policies.

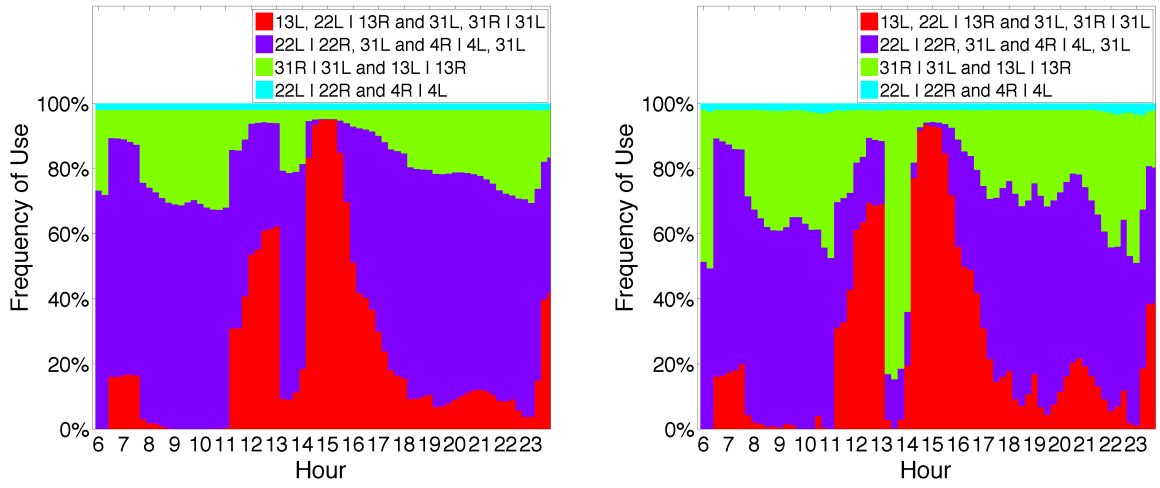

(a) $\tau_I = 3$ min

(b) Differentiated $\tau_I^{RC_1,RC_2}$

Figure 11: Frequency of use of runway configurations with uniform versus differentiated values of τ_I

In addition to selecting runway configurations, as shown in Figures 10 and 11, the model introduced in this paper controls the arrival and departure service rates at each period of the day. The frequency of these decisions is shown in Table 4 for seven different periods and the six most frequently used configurations. Note that, after a particular runway configuration has been selected, any variations in selected arrival and departure service rates are solely motivated by differences in prior stochastic queue evolution, and depend neither on the runway configuration previously in use nor on wind conditions. As seen in the table, for some periods of the day (*e.g.*, at 6:45 and 15:15) the choice of arrival and departure service rates depends only weakly on the prior evolution of arrival and departure queues. In these cases, the main control exercised is the selection of the runway configuration, primarily determined by previous runway configurations and wind-related constraints, but the optimal balance of arrivals and departures does not vary substantially from one sample to another. For instance, the decision-maker selects most frequently the largest arrival rate available at 15:15 and an arrival rate equal to 8 or 9 landings per 15-minute period at 6:45. In contrast, in many other cases, the optimal balance of arrivals and departure is highly variable and depends on the observed extent of congestion at the time of the decision (*e.g.*, at 7:45, 10:30, 11:45, 17:00 and 22:15). In such cases, both the optimal runway configuration and the optimal arrival and departure service rates might depend on the prior evolution of the system.

These results show the path-dependency of the optimal policy. At each period, the optimal runway configuration and service rates depend on the state of the system at the time of the decision (Figure 9), which itself depends on previous decisions and on the prior evolution of the system. This includes, first, some deterministic components, such as the runway configuration in

Table 4: Policy frequency for six different periods of the day

Policy			Period t						
RC_t	μ_t^a	μ_t^d	6:45	7:45	10:30	11:45	15:15	17:00	22:15
$13L, 22L\|13R$	16	8.0	–	–	2%	4%	42%	3%	–
	15	8.5	–	–	–	5%	–	–	–
	14	9.0	–	–	–	8%	–	4%	1%
	13	9.3	–	–	–	4%	–	1%	–
	11	9.9	–	–	–	5%	–	7%	1%
	10	10.1	–	–	–	4%	–	9%	2%
	9	10.2	–	–	–	2%	–	3%	3%
$31L, 31R\|31L$	16	5.2	–	–	–	2%	52%	8%	–
	12	7.7	–	–	–	3%	–	–	–
	11	8.3	–	–	–	3%	–	–	–
	7	10.7	–	–	–	1%	–	3%	–
$22L\|22R, 31L$	13	8.8	–	8%	5%	8%	–	9%	4%
	12	9.4	–	5%	1%	3%	–	4%	7%
	10	10.5	–	7%	2%	3%	–	5%	4%
	9	11.0	49%	10%	7%	2%	–	11%	8%
	8	11.3	–	3%	–	–	–	–	–
	7	11.7	1%	7%	7%	1%	–	3%	5%
	6	12.0	–	3%	3%	–	–	1%	2%
	5	12.3	–	1%	3%	–	–	–	1%
	4	12.6	–	1%	6%	–	–	–	1%
$4R\|4L, 31L$	13	8.2	–	4%	2%	4%	–	6%	2%
	10	10.0	–	5%	4%	4%	–	7%	6%
	8	10.8	20%	2%	3%	1%	–	1%	3%
	7	11.2	2%	3%	3%	1%	–	1%	2%
	6	11.6	–	2%	3%	–	–	1%	2%
	4	12.4	–	1%	4%	–	–	–	2%
$31R\|31L$	13	8.3	–	3%	1%	2%	3%	2%	1%
	10	10.0	–	3%	1%	1%	–	1%	2%
	9	10.5	4%	5%	4%	1%	–	1%	5%
	8	10.8	13%	–	1%	–	–	–	–
	7	11.2	2%	3%	5%	1%	–	–	3%
	4	12.1	–	1%	5%	–	–	–	1%
$13L\|13R$	7	11.1	6%	2%	1%	–	–	–	3%
	6	11.4	–	1%	6%	–	–	–	2%

use. It also includes exogenous stochastic components, such as the evolution of weather and wind conditions. For instance, configuration $4L|4L, 31L$ achieves a slightly lower departure throughput

than configuration $22L|22R, 31L$. Nonetheless, it may be used when the balance of arrivals and departures requires the use of a configuration with two arrival runways and one departure runway and when strong winds from the North prevent runways $22L$ and $22R$ from being used. Last, and perhaps most important, optimal policies depend on endogenous stochastic components, such as the length of the arrival and departure queues. These lengths depend on previous decisions, as well as on the stochastic evolution of the system. This stochasticity gives rise to some variability in the optimal control at any period of the day (see Figures 10 and 11 and Table 4): both the runway configurations and the arrival and departure service rates depend on prior system evolution. This underscores the importance of considering queue stochasticity and its endogeneity to operating decisions within our decision-making framework, because of the impact this may have on optimal decisions. We further estimate the benefits of accounting for queue stochasticity in § 5.2.

4.3 Sensitivity of Arrival and Departure Queues to Model Parameters

We have performed several sensitivity analyses to evaluate how the optimal policies and the optimal arrival and departure queue lengths vary with several model parameters. First, increases in the relative cost of arrival queuing, α, lead to the selection of policies that increase the arrival throughput at the expense of the departure throughput and therefore to shorter expected arrival queues and longer expected departure queues. Variations in α from 1 to 2 induce changes in peak expected arrival queue length on the order of 2 to 3 aircraft in queue (*i.e.*, over 30%) and changes in peak expected departure queue length on the order of 1 to 2 aircraft in queue (*i.e.*, 5% to 10%). This difference might be due to the slope of the Operational Throughput Envelope at JFK being lower than 1 (Figure 6), so variations in arrival rates induce smaller variations in departure rates.

As well, variations in the duration of idleness following a runway configuration change, τ_I, induce changes in the efficiency of operations and in the optimal policy (see § 4.2), thus in optimal arrival and departure queues. As τ_I increases from 0 to 15 minutes, the expected arrival queue length might increase by 1 to 2 aircraft and the expected departure queue length might increase by 2 to 3 aircraft. This translates into increases in the optimal expected congestion costs. Table 5 reports the optimal total congestion costs for the 9 days considered and for $\tau_I = 0, 5, 10$ and 15 min. Note that the total expected costs increase by 25% to 40% when τ_I increases from 0 to 15 minutes. Therefore, the efficiency with which airports can switch between runway configurations has a significant impact on expected airport congestion costs.

5 Performance Evaluation

We now quantify the benefits resulting from the control of runway configurations and of arrival and departure service rates developed in this paper. We first compare the optimal policy to two advanced heuristics that aim to imitate typical operating decisions made in practice. We then

Table 5: Expected total congestion costs for different values of τ_I

		Expected total cost			
Day	Flights	$\tau_I = 0$ min	$\tau_I = 5$ min	$\tau_I = 10$ min	$\tau_I = 15$ min
02/04	1,027	Baseline	+18.15%	+28.37%	+37.16%
01/10	1,059	Baseline	+17.57%	+29.13%	+39.35%
02/08	1,085	Baseline	+18.31%	+29.93%	+39.23%
01/25	1,097	Baseline	+17.38%	+27.79%	+36.38%
09/18	1,113	Baseline	+13.67%	+23.52%	+32.17%
10/15	1,125	Baseline	+15.93%	+25.45%	+33.81%
06/01	1,133	Baseline	+14.43%	+24.19%	+34.18%
07/07	1,160	Baseline	+10.58%	+17.38%	+24.89%
05/25	1,172	Baseline	+12.19%	+19.22%	+26.23%

compare it to an alternative model based on deterministic queue dynamics to quantify the benefits of integrating queue stochasticity into the decision-making framework.

5.1 Comparison of the Optimal Policy to Heuristics

In this section, we compare the optimal policies obtained with the DP model to two heuristic policies. The heuristics can be viewed as representative of the kind of "reasonably smart" operating policies one might apply in practice, in the absence of an advanced model such as the DP model presented here. If our model can outperform the heuristics by a significant margin, this would suggest that large congestion cost savings might result from the model's implementation as a tool for tactical decision-making. Comparisons of the associated congestion costs provide estimates of the potential savings that may result from such implementation.

Note that, ideally, one would compare the policies recommended by the model to actual decisions made in practice. However, such comparison is complicated by several factors. First, identifying arrival and departure queue lengths and service rates from available databases is subject to significant uncertainty. Second, little data on real-time information available to decision-makers in practice (*e.g.*, dynamic schedule updates) is reported. Third, establishing statistically reliable comparisons and isolating the benefits of our DP model requires the consideration of many days of operations, which is complicated by the stochasticity of the system and variations in the schedules of flights and operating conditions from one day to another. For these reasons, we approximate actual decisions through the two heuristics described below. This approach is similar to the one adopted in the literature [8, 5]. Note, however, that some differences with actual decisions might also arise from practical factors that were not included in the model. Discussions with air traffic managers are therefore required to design iterative improvements of our model and of its implementation.

The two heuristics we consider were developed from discussions with air traffic managers at JFK.

Both adjust the arrival rate as a function of arrival demand, which seems to be common practice at the busiest airports. This might be motivated by the fact that, at JFK, the departure rate is not very sensitive to the arrival rate. Indeed, as previously discussed, the departure rates shown by the Operational Throughput Envelopes of the main runway configurations at JFK decrease by less than 1 for every unit increase in the arrival rates (Figure 6). Therefore, increasing the arrival rate to match arrival demand induces a relatively small loss in departure throughput. Moreover, this might be motivated by practical reasons as well, since it is more challenging operationally to hold arriving aircraft in queue in the air than to hold departing aircraft in queue on the ground. We describe briefly the two heuristics below and in more detail in the Appendix.

The first heuristic assumes no cost of changing runway configurations. At the beginning of each period, the decision-maker computes the *effective arrival demand*, defined as the expected number of aircraft that will request to land in the period. It is simply equal to the sum of the arrival queue at the beginning of period t, *i.e.*, a_{t-1}, and the expected number of aircraft that will join the arrival queue in period t, *i.e.*, x_t. He then attempts to satisfy arrival demand by selecting an arrival rate equal to the effective arrival demand, if possible. If the maximal arrival rate of each of the runway configurations that can be used under observed wind conditions is smaller than the effective arrival demand, then he selects the largest arrival rate that can be possibly chosen. He then operates in the runway configuration that maximizes the departure service rate for the selected arrival rate.

The second heuristic relies on a similar approach except that a large cost of switching runway configurations is assumed. The decision-maker does not change runway configurations unless he is forced to do so, because of changing wind conditions. If the current runway configuration can still be used for the next period, then he chooses the arrival rate that matches the effective arrival demand as closely as possible and the departure rate is subsequently determined by the Operational Throughput Envelope of the runway configuration. If, however, the current runway configuration can no longer be used, then he follows the policy determined according to the first heuristic.

Table 6 reports the relative difference between the optimal expected congestion costs and the expected congestion costs resulting from the application of each of these two heuristics, for different values of the duration of idleness τ_I. As expected, Heuristic 2 performs better for the larger values of τ_I (*e.g.*, $\tau_I = 10$ min), while Heuristic 1 performs better for the smaller values of τ_I (*e.g.*, $\tau_I = 0$ min). This is consistent with the design of these heuristics. But in all the cases considered ($\tau_I = 0$ min, $\tau_I = 5$ min and $\tau_I = 10$ min), the *better* of the two heuristics results in significantly greater congestion costs than the optimal policy, by an estimated 20% to 30%. These results suggest that the optimal control might result in substantial cost savings. Finally, the estimated 20% to 30% reduction in congestion costs is substantially larger than the 1% to 2% error of the one-step look-ahead algorithm implemented in § 3.3. This suggests that, when real-time disturbances are considered, the approximate scheme developed in this paper would still result in significant operational improvements compared to the two advanced heuristics considered in this section.

Table 6: Relative error of heuristics

			Heuristic 1		Heuristic 2	
Day	Flights	Exact	$\tau_I = 0$ min	$\tau_I = 5$ min	$\tau_I = 5$ min	$\tau_I = 10$ min
02/04	1,027	Baseline	+35.18%	+56.61%	+45.28%	+36.88%
01/10	1,059	Baseline	+35.34%	+75.58%	+51.48%	+41.82%
02/08	1,085	Baseline	+37.60%	+68.60%	+46.84%	+37.17%
01/25	1,097	Baseline	+34.60%	+63.13%	+44.37%	+35.79%
09/18	1,113	Baseline	+28.23%	+57.18%	+37.86%	+29.76%
10/15	1,125	Baseline	+30.19%	+57.29%	+38.13%	+30.70%
06/01	1,133	Baseline	+29.65%	+65.19%	+45.97%	+37.75%
07/07	1,160	Baseline	+19.07%	+41.27%	+29.95%	+25.01%
05/25	1,172	Baseline	+25.02%	+43.70%	+31.48%	+26.08%

The comparison of the optimal control to heuristics suggests that the joint control of runway configurations and of arrival and departure service rates can improve the efficiency of airport operations substantially. As mentioned in the introduction, the annual costs of air traffic delays in the United States were estimated at over $30 billion for the year 2007 [1], 50% to 75% of which are attributed to mismatches between demand and capacity [6]. Given the disproportionate distribution of delays across airports and the propagation of these delays through the National Aviation System, the implementation of the control developed in this paper at a few of the busiest airports in the United States could generate very significant cost savings for airlines, passengers and society.

5.2 Benefits of the Integration of Queue Stochasticity

Finally, we quantify the benefits of integrating the stochasticity of queue dynamics into the decision-making framework. To this purpose, we implement an alternative version of the model developed in this paper, but with deterministic queue dynamics. In this case, the queue transition probabilities (see § 2.4.1) are simply defined as follows:

$$Q^t_{m,n} = \begin{cases} 1, & \text{if } n = m + \lambda_t - \mu_t \\ 0, & \text{otherwise} \end{cases} \tag{8}$$

Using (8), we derive the optimal policy under deterministic queue dynamics and we compare it to the optimal policy based on stochastic queue dynamics that we obtained previously. Note that both policies consider the same model of weather and wind dynamics. Any difference is therefore due to the consideration, or not, of queue stochasticity. We then simulate the evolution of the system resulting from the application of the optimal deterministic and stochastic policies, under stochastic queue dynamics.

We compare in Table 7 the congestion costs obtained with each of the two policies, for different

values of τ_I. These results suggest that accounting for the stochasticity of queue dynamics in the design of the operating policy might yield significant congestion cost savings, which we estimate from our tests at 5% to 20%. Note that the benefits of integrating queue stochasticity seem larger with the larger values of τ_I (*e.g.*, $\tau_I = 5$ min and $\tau_I = 10$ min) than with $\tau_I = 0$ min. This might be explained by the fact that, with $\tau_I = 0$, the deterministic model is able to atone, to some extent, for its lack of consideration of stochasticity. It does this by making more frequent changes (at no cost) to runway configurations in response to unexpected changes in the arrival and departure queues.

Table 7: Relative performance of the optimal deterministic and stochastic policies

		$\tau_I = 0$ min		$\tau_I = 5$ min		$\tau_I = 10$ min	
Day	Flights	Stochastic	Determ.	Stochastic	Determ.	Stochastic	Determ.
02/04	1,027	Baseline	+9.06%	Baseline	+16.70%	Baseline	+14.31%
01/10	1,059	Baseline	+8.24%	Baseline	+14.25%	Baseline	+11.92%
02/08	1,085	Baseline	+8.05%	Baseline	+16.30%	Baseline	+12.51%
01/25	1,097	Baseline	+7.91%	Baseline	+16.45%	Baseline	+13.22%
09/18	1,113	Baseline	+6.70%	Baseline	+13.77%	Baseline	+11.48%
10/15	1,125	Baseline	+7.76%	Baseline	+17.16%	Baseline	+14.92%
06/01	1,133	Baseline	+7.73%	Baseline	+18.19%	Baseline	+16.27%
07/07	1,160	Baseline	+5.60%	Baseline	+11.50%	Baseline	+11.42%
05/25	1,172	Baseline	+6.58%	Baseline	+13.49%	Baseline	+12.84%

In conclusion, the stochasticity of queue dynamics has a significant impact on the optimal policy. Ignoring this stochasticity can result in significant operating inefficiencies, estimated at 5% to 20%. This is consistent with the path-dependency of the optimal policy shown in § 4.1.

6 Conclusion

In this paper, we presented an original decision-making framework that dynamically controls runway configurations and the arrival and departure service rates at a major airport while taking into account the stochasticity of arrival and departure queue dynamics and of operating conditions. This addresses the problem of dynamically allocating airport capacity to arriving and departing aircraft under operating uncertainty. We developed an efficient Dynamic Programming (DP) formulation that minimizes airport congestion costs and embeds a realistic stochastic model of queue dynamics and of weather and wind-related uncertainty.

We applied the exact DP algorithm to a realistic setting at JFK Airport and showed that, based on information available before a particular day of operations, the optimal *a priori* operating policy for that day can be obtained within reasonable computational times. However, during the day in question, the policy thus obtained may no longer be optimal due to unforeseen disturbances, such

as schedule updates or changes in the weather forecast. To address this issue, we implemented a one-step look-ahead approximate algorithm that greatly speeds up execution of the DP. Results suggest that this two-step approximation scheme yields near-optimal policies. The fast approximate algorithm therefore enables the on-line implementation of our model using real-time information.

The application of the model at JFK yielded several insights. First, optimal policies are path-dependent in the sense that they depend on the prior evolution of the system, including prior decisions and the stochastic evolution of arrival and departure queues over the day. This underscores the impact of system stochasticity on optimal policies. As a result, we showed that integrating the stochasticity of queue dynamics into the decision-making framework can yield significant congestion cost savings, estimated at 5% to 20%. Moreover, comparisons of optimal policies to two advanced heuristics, aimed to imitate actual operating procedures, suggest that congestion costs might be significantly reduced through the control of runway configurations and of service rates developed in this paper. Our results at JFK indicate the potential for congestion cost savings of as much as 20% to 30% at the busiest airports.

The model and the algorithms presented provide an effective decision-making tool to mitigate airport congestion at the tactical level. Its implementation may provide substantial operational benefits to airport stakeholders. Moreover, the model provides a better understanding of how airport capacity utilization procedures depend on the schedule of flights and on the stochastic evolution of the arrival and departure queues at the airport. This can be used to integrate the interdependencies between flight schedules, airport delays and airport operating procedures into macroscopic models of airport congestion at the strategic level. Such integration could, in turn, improve the predictive abilities of these models. In ongoing work, we are using these tools to develop an integrated approach to airport congestion mitigation that jointly optimizes the rescheduling of flights through schedule coordination at the strategic level and the utilization of airport capacity at the tactical level [18].

Acknowledgments

This research was supported in part by the Federal Aviation Administration as a NEXTOR-2 project. The help of Ioannis Simaiakis in getting the Operational Throughput Envelopes from JFK, is gratefully acknowledged. The authors thank the anonymous reviewers for their insightful comments. The authors are solely responsible for any errors or opinions expressed herein.

7 Appendix: Algorithmic Description of the Heuristics

The algorithmic implementation of the two heuristics used in § 5.1 is presented below. They consist of computing, at the beginning of each time period t, the effective arrival demand, denoted by ad_t and defined as the expected number of aircraft that will request to land in period t. In other words,

$ad_t = a_{t-1} + x_t$. In the first heuristic (Algorithm 1), we determine the set of configurations that can match arrival demand as well as possible and, among all the configurations that satisfy this requirement, we select the one that maximizes the departure service rate. In the second algorithm (Algorithm 2), we assume that the configuration does not change unless it is no longer feasible to use it—because of a change in wind conditions. Again, the arrival rate is selected to match as closely as possible arrival demand.

Algorithm 1 Heuristic 1: Arrival priority and no cost of runway configuration changes

for $t = 1, ..., T$ **do**
  for a_{t-1} **do**

- Compute effective arrival demand: $ad_t = a_{t-1} + x_t$

    for wc_t, ws_t **do**
      for $rc \in \mathcal{RC}(ws_t)$ **do**

- Define candidate arrival rate with rc: $ar_t(rc) = \min\left(A_{rc,wc_t}, ad_t\right)$

      end for

- Determine the set of candidate runway configurations $\mathcal{RC}_{ar_t}(ws_t) \subset \mathcal{RC}(ws_t)$ that minimize the quantity $|ad_t - ar_t(rc)|$ and define new arrival rate μ_t^a as the corresponding value of $ar_t(rc), rc \in \mathcal{RC}_{ar_t}(ws_t)$
- Choose runway configuration $RC_t = \arg\max_{rc \in \mathcal{RC}_{ar_t}(ws_t)} \left\{\Phi_{rc,wc_t}\left(\mu_t^a\right)\right\}$
- Define new departure rate: $\mu_t^d = \Phi_{RC_t,wc_t}\left(\mu_t^a\right)$

    end for
  end for
end for

Algorithm 2 Heuristic 2: Arrival priority and large cost of runway configuration changes

for $t = 1, ..., T$ **do**
  for RC_{t-1} **do**

- Determine the set of wind states $\mathcal{WS}_{RC_{t-1}}$ in which RC_{t-1} can be feasibly used

    for $ws_t \in \mathcal{WS}_{RC_{t-1}}$ **do**

- Choose same runway configuration: $RC_t = RC_{t-1}$

      for a_{t-1}, wc_t **do**

- Compute effective arrival demand: $ad_t = a_{t-1} + x_t$
- Define new arrival rate: $\mu_t^a = \min\left(A_{RC_t,wc_t}, ad_t\right)$
- Define new departure rate: $\mu_t^d = \Phi_{RC_t,wc_t}\left(\mu_t^a\right)$

      end for
    end for
    for $ws_t \notin \mathcal{WS}_{RC_{t-1}}$ **do**

- Choose policy from Heuristic 1 in all states

    end for
  end for
end for

References

[1] M. Ball, C. Barnhart, M. Dresner, M. Hansen, K. Neels, A. Odoni, E. Peterson, L. Sherry, A. Trani, and B. Zou. Total Delay Impact Study. Technical report, National Center of Excellence for Aviation Operations Research, 2010.

[2] Richard Bellman. *Dynamic Programming*. Princeton University Press, Princeton, NJ, 1957.

[3] D. Bertsekas. *Dynamic Programming and Optimal Control*, volume I. Athena Scientific, 3rd edition, 2005.

[4] D. Bertsekas and J. Tsitsiklis. *Neuro-Dynamic Programming*. Athena Scientific, 1996.

[5] D. Bertsimas, M. Frankovich, and A. Odoni. Optimal Selection of Airport Runway Conigurations. *Operations Research*, 59(6):1407–1419, 2011.

[6] Bureau of Transportation Statistics. TranStats. Accessed March 26, 2013. www.transtats.bts.gov, 2013.

[7] R. de Neufville and A. Odoni. *Airport Systems: Planning, Design and Management*. McGraw-Hill, 2nd edition, 2013.

[8] P. Dell'Olmo and G. Lulli. A Dynamic Programming Approach for the Airport Capacity Allocation Problem. *IMA Journal of Management Mathematics*, 14(3):249, 2003.

[9] Federal Aviation Administration. Airport Design. Advisory Circular 150/5300-13A, 2012.

[10] Federal Aviation Administration. Aviation Performance Metrics (APM) database. Accessed April 4, 2013. Available at: https://aspm.faa.gov/apm, 2013.

[11] Federal Aviation Administration. NextGen Implementation Plan. Technical report, 2013.

[12] E. Gilbo. Airport Capacity: Representation, Estimation, Optimization. *IEEE Transactions on Control Systems Technology*, 1(3):144–154, 1993.

[13] E. Gilbo. Optimizing Airport Capacity Utilization in Air Traffic Flow Management subject to Constraints at Arrival and Departure Fixes. *IEEE Transactions on Control Systems Technology*, 5(5):490–503, 1997.

[14] E. Gilbo and K. Howard. Collaborative Optimization of Airport Arrival and Departure Traffic Flow Management Strategies for CDM. In *3rd USA/Europe Air Traffic Management R&D Seminar*, 2000.

[15] W. Hall. *Efficient Capacity Allocation in a Collaborative Air Transportation System*. PhD thesis, Massachusetts Institute of Technology, 1999.

[16] M. Hansen, A. Odoni, D. Lovell, T. Nikoleris, and K. Vlachou. Use of Queuing Models to Estimate Delays Savings from 4D Trajectory Precision. In *8th USA/Europe Air Traffic Management R&D Seminar*, 2009.

[17] A. Jacquillat. A Queuing Model of Airport Congestion and Policy Implications at JFK and EWR. Master's thesis, Massachusetts Institute of Technology, 2012.

[18] A. Jacquillat and A. Odoni. Congestion Mitigation through Schedule Coordination at JFK: An Integrated Approach. *ESD Working Paper Series*, Available at http://esd.mit.edu/WPS/2013/esd-wp-2013-17.pdf, 2013.

[19] P. Kivestu. Alternative Methods of Investigating the Time Dependent M/G/k Queue. Master's thesis, Massachusetts Institute of Technology, 1974.

[20] L. Li and J. P. Clarke. A Stochastic Model of Runway Configuration Planning. In *AIAA Guidance, Navigation, and Control Conference*, 2010.

[21] P. B. Liu, M. Hansen, and A. Mukherjee. Scenario-based Air Traffic Flow Management: From Theory to Practice. *Transportation Research Part B*, 42:685–702, 2008.

[22] D. Lovell, A. Chruchill, A. Odoni, A. Mukherjee, and M. Ball. Calibrating Aggregate Models of Flight Delays and Cancellation Probabilities at Individual Airports. In *7th USA/Europe Air Traffic Management R&D Seminar*, 2007.

[23] T. Nikoleris and M. Hansen. Queueing Models for Trajectory-Based Aircraft Operations. *Transportation Science*, 46(4):501–511, 2012.

[24] N. Pyrgiotis, K. Malone, and A. Odoni. Modelling Delay Propagation within an Airport Network. *Transportation Research Part C*, 27:60–75, 2013.

[25] N. Pyrgiotis and A. Odoni. On the Impact of Scheduling Limits: A Case Study at Newark International Airport. *Transportation Science*, Forthcoming, 2014.

[26] N. Pyrgiotis and I. Simaiakis. An Analytical Queuing Model of Airport Departure Processes for Taxi Out Time Prediction. In *AIAA Aviation Technology, Integration, and Operations*, 2010.

[27] V. Ramanujam and H. Balakrishnan. Estimation of Maximum-Likelihood Discrete-Choice Models of the Runway Configuration Selection Process. In *American Control Conference*, 2011.

[28] I. Simaiakis. *Analysis, Modeling and Control of the Airport Departure Process*. PhD thesis, Massachusetts Institute of Technology, 2012.

[29] I. Simaiakis and H. Balakrishnan. Probabilistic Modeling of Runway Inter-departure Times. *AIAA Journal of Guidance, Control and Dynamics*, 2014.

[30] P. Swaroop, B. Zou, M. Ball, and M. Hansen. Do More US Airports Need Slot Controls? A Welfare Based Approach to Determine Slot Levels. *Transportation Research Part B*, 46(9):1239–1259, 2012.

[31] V. Vaze and C. Barnhart. Modeling Airline Frequency Competition for Airport Congestion Mitigation. *Transportation Science*, 46(4):512–535, 2012.

[32] C. Weld, M. Duarte, and R. Kincaid. A Runway Configuration Management Model with Marginally Decreasing Transition Capacities. *Advances in Operations Research*, 2010.